First retrievals of methane isotopologue, CH_3D, from FTIR ground-based observations

W. Bader[1,2], K. Strong[1], K. Walker[1], E. Buzan[3]

[1]Department of Physics, University of Toronto, Toronto, ON, Canada

[2]Institute of Astrophysics and Geophysics, University of Liège, Liège, Belgium

[3]Department of Chemistry and Biochemistry, Old Dominion University, Norfolk, Virginia, USA

INTRODUCTION & MOTIVATION

Atmospheric methane (CH_4), with a lifetime of 8-10 years, is the second most important anthropogenic greenhouse gas (radiative forcing of 0.97 ± 0.23 $W.m^{-2}$, RF of CO_2 in 2011: 1.68 ± 0.35 $W.m^{-2}$; Stocker et al., 2013). Approximately one-fifth of the increase in radiative forcing by human-linked greenhouse gases since 1750 is due to methane (Nisbet et al., 2014). Identified emission sources include anthropogenic (coal mining, oil and gas exploitation, rice cultures, domestic ruminant animals, biomass burning, and waste management) and natural contributions (wetlands, termites, methane hydrates and ocean). Due to its sinks, methane plays a role of regulator of hydroxyl radical (OH) and of ozone precursor in the troposphere (Montzka et al., 2011) while in the stratosphere, it acts as a source of water vapor and as a sink for chlorine atoms which reduces the rate of ozone depletion. Atmospheric methane concentrations have reached a new high at 1845 ± 2 ppb, accounting for an increase of 256 % since pre-industrial times (WMO, 2016). In the last ten years, methane has been on the rise again at rates of ~0.3%/year (e.g., Bader et al., 2017), after a period of stabilization of about 5 years. This recent increase is not fully understood due to remaining uncertainties in the methane budget, influenced by numerous anthropogenic and natural emission sources. In order to examine the cause(s) of this increase, we focus on one of the two main methane isotopologues, i.e. **CH_3D**. Methane isotopologues are emitted in the atmosphere with different ratio depending on the emission processes involved (Rigby et al., 2012). As heavier isotopologues will react more slowly than $^{12}CH_4$, each isotopologue will be depleted from the atmosphere at a specific rate depending on the removal process (Saueressig et al., 2001). Methane isotopologues are therefore good tracers of the methane budget.

INSTRUMENTATION & DATASET

First development and optimization of the retrieval strategy for CH_3D from ground-based FTIR (Fourier Transform infrared) solar observations with the SFIT-4 algorithm.

Toronto, ON, Canada (Wiacek, et al., 2007)

Bomem DA8 Fourier Transform Spectrometer

~1430 days of observations since May 2002

Eureka, NU, Canada (Batchelor et al., 2009, Fu et al., 2007)

Bruker IFS-125 HR Fourier Transform Spectrometer

~760 days of observations since July 2006

Portable Atmospheric Research Interferometric Spectrometer for the InfraRed

~240 days of spring observations at Eureka since 2004

Jungfraujoch, Switzerland (Zander et al., 2008)

Bruker 120-HR : ~2590 days of observations since 1990

A PRIORI MIXING RATIO PROFILES

CH_3D vertical mixing ratio information is obtained from a Whole Atmosphere Community Climate Model (WACCM v.4, Marsh et al., 2013) simulation run as a standalone model with a resolution of 4×5° (latitude x longitude) and 66 vertical levels (Buzan et al., 2016). The model was run as a perpetual year 2000 for a total of 20 years: 17 years of spin-up time followed by 3 years that were averaged to produce a single a priori mixing ratio profile per station. Water vapor mixing ratio profiles from daily averages NCEP reanalysis and ozone monthly averaged profiles over the years 1980-2020 from a WACCM simulation (V6) are used as a priori.

SPECTROSCOPIC LINELISTS

In order to minimize residuals, the best combination of available spectroscopic linelists has been determined :

CH_4 and isotopologues

Spectroscopic linelist for GGG2014, TCCON data archive developed by Toon et al. (2014)

Water vapour

Experimental linelist of water vapor line parameters developed by Loos et al. (2017a and 2017b)

Interfering species

The HITRAN 2008 compilation (Rothman et al., 2009), for other interfering species, including O_3

RETRIEVAL CONSTRAINT

The retrieval strategy is based on an altitude constrained Tikhonov L_1 approach similar to the one recommended by the Network for the Detection of Atmospheric Composition Change for the retrieval strategy of $^{12}CH_4$.

The smoothing constrained is defined as:

$$\boldsymbol{R} = \alpha\, \boldsymbol{L_1}^{\mathrm{T}}\, \boldsymbol{T}\, \boldsymbol{L_1}$$

where $\boldsymbol{L_1}$ is the constraint operator, $\boldsymbol{T}$ expresses the altitude constraint associated to the retrieval vertical grid, and α is the strength of the constraint. α is determined by minimizing the total error (measurement + smoothing error) as illustrated in Steck et al. (2002).

Figure 1 illustrates the measurement and smoothing errors computed according to the formalism of Rodgers (1990) with respect to α. The errors displayed in Fig. 1 are averaged errors over one year (2010) of retrievals from FTIR observations collected at Eureka.

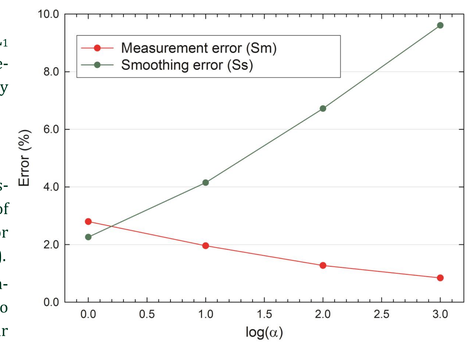

Figure 1

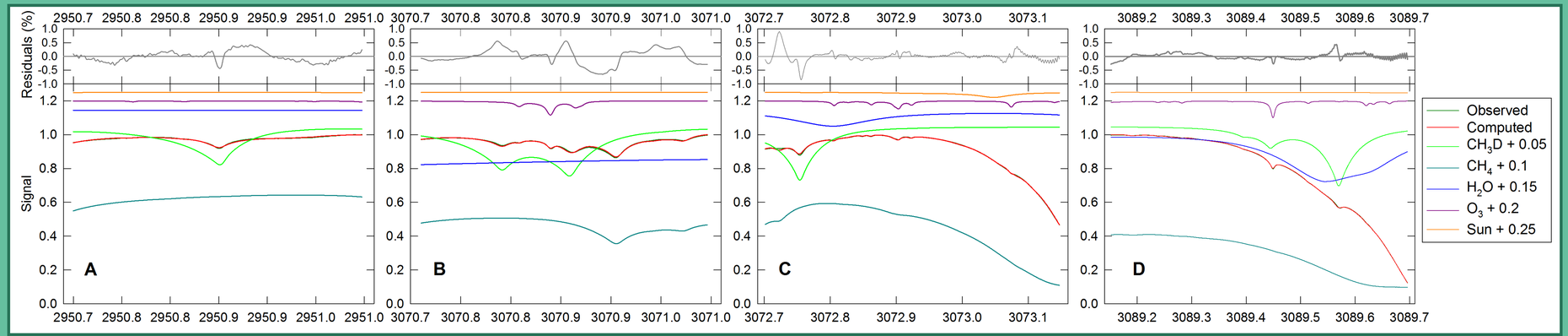

Figure 2 - Averaged observed (in green) and calculated (in red) spectra (lower frame) as well as residuals in % (grey line in higher frame) derived from a representative set of observations (222 spectra) collected at Toronto during 2005. The individual contributions of each interfering gas have been vertically displaced for clarity. Window limits are (**A**) 2950.7 - 2951, (**B**) 3070.71 - 3073.15, (**C**) 3072.7 - 3073.15, (**D**) 2089.15 - 2089.7 cm^{-1}.

THE BENEFIT OF 4 WINDOWS (see Figure 2 for letter codes) ?

Figure 3 illustrates the error budget (Rodgers, 1990) depending on the use of 4 windows for both Toronto and Eureka measurements. Using 4 windows (A+B+C+D, in pink) allows us to simultaneously decrease measurement and smooothing errors while improving the Degrees of Freedom for Signal (DOFS) reaching a value as high as 1.43 (Toronto) and 3.95 (Eureka), see Fig. 6.

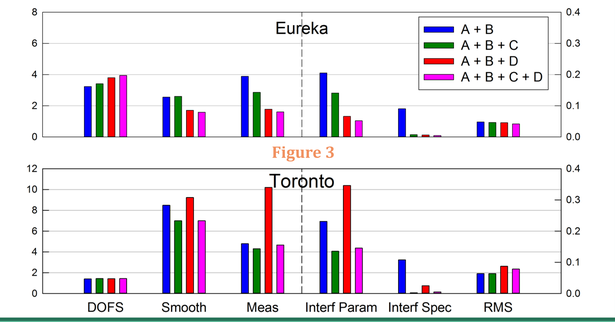

Figure 3

WATER VAPOR SPECIFIC WINDOW ?

In order to better identify the water vapor interferences, a H_2O specific window (2941.65 –2941.89 cm^{-1}, Bader et al., 2017) is tested as the fifth window.

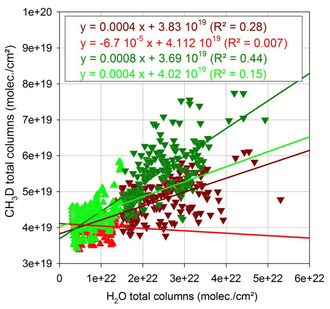

Figure 4 - Correlation between CH_3D and H_2O retrieved total columns with (in red) and without the use of the "H_2O" window (in green).

While combining the 4 windows reduces smoothing and measurement errors and increases DOFS (see Fig. 3), overlapping of H_2O and CH_3D absorption lines in windows **C** and **D** (see Fig. 2), may result in a misinterpretation of the CH_3D total columns for humid days.

CH_4 PROFILE RETRIEVAL ?

To assess isotopic ratios of CH_4 through δ-D computation, it is necessary to simultaneously retrieve precise and accurate $^{12}CH_4$ total columns along with CH_3D. We observe a systematic bias between the retrieved and the archived CH_4 columns of approximately 11.2 and 11.5 % respectively with a scaled or retrieved CH_4 profile. Retrieving the CH_4 profile increases smoothing, measurement and interference errors of about 0.02 %.

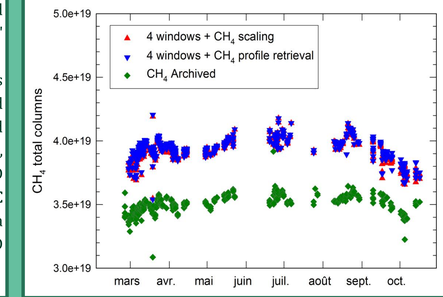

Figure 5 - CH_4 total column time series as retrieved from Eureka observations with (blue) or without CH_4 profile retrieval (red) along with CH_4 as archived on the NDACC website. www.ndacc.org

ERROR BUDGET AND INFORMATION CONTENT

Figure 6 illustrates averaging kernels, eigen vectors and associated eigen values for Eureka and Toronto, averaged over 2010 and 2005 and with DOFS of 1.43 and 3.95, respectively.

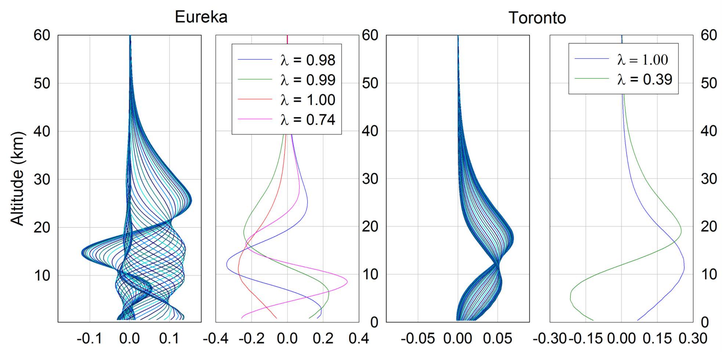

REFERENCES

Bader, W. et al., 2017, Atmos. Chem. Phys., 10.5194/acp-17-2255-2017

Batchelor, R. et al., 2009, J. Atmos. Ocean. Technol., 10.1175/2009JTECHA1215.1

Buzan, E. M. et al., 2016, Atmos. Meas. Tech., 10.5194/amt-9-1095-2016

Fu, D. et al., 2007, J. Quant. Spectrosc. Radiat. Transf., 10.1016/j.jqsrt.2006.05.006

Loos J. et al., 2017a, J. Quant. Spectrosc. Radiat. Transf., 10.1016/j.jqsrt.2017.02.013

Loos J. et al., 2017b, J. Quant. Spectrosc. Radiat. Transf., 10.1016/j.jqsrt.2017.03.033

Marsh, D. R., et al., 2013, J. Clim., 10.1175/JCLI-D-12-00558.1

Montzka, S.A. et al., 2011, Science, 10.1126/science.1197640

Nisbet, E.G., et al., 2014, Science, 10.1126/science.1247828

Rigby, M., et al., 2012, J. Geophys. Res, 10.1029/2011JD017384

Rodgers, C.D., 1990, J. Geophys. Res., 10.1029/JD095iD05p05587

Rothman, L. S. et al., 2009, J. Quant. Spectrosc. Radiat. Transf., 10.1016/j.jqsrt.2009.02.013

Saueressig, G. et al., 2011, J. Geophys. Res., 10.1029/2000JD000120

Steck, T. et al., 2002, Appl. Opt., 10.1364/AO.41.001788

Stocker, T., 2013, 5th IPCC Report, Working Group I

Toon, G. C., 2014, doi:10. 14291/tccon.ggg2014.atm.R0/1221656

Wiacek, A., et al., 2007, J. Atmos. Ocean. Technol., 10.1175/JTECH1962.1

World Meteorological Organization, Greenhouse gas bulletin, N°12, October 2016

Zander, R., et al., 2008, Science of the Total Env.,10.1016/j.scitotenv.2007.10.018

Author contact : wbader@atmosp.physics.utoronto.ca

Acknowledgments - W. Bader has received funding from the European Union's Horizon2020 research and innovation programme under the Marie Sklodowska-Curie grant agreement n°704951, and from the University of Toronto through a Faculty of Arts & Science Postdoctoral Fellowship Award.